Iranian Journal of Science and Technology, Transactions of Civil Engineering (2020) 44:1171–1177
https://doi.org/10.1007/s40996-019-00309-4

RESEARCH PAPER

Research on Strain Rate Effect of the Mechanical Properties of Graphene Sheet Containing Randomly Distributed Defects

Yingjing Liang[1] · **Shi Huan**[2]

Received: 25 October 2018 / Accepted: 3 September 2019 / Published online: 13 September 2019

Abstract
Strain rate effects on the mechanical properties of graphene sheets (GSs) contain randomly distributed defects investigated by molecular dynamics simulations, and the results have been discussed. The strain rate has a significant effect on the tensile strength, while fracture strain and failure mechanism of GSs and elastic modulus are insensitive to the strain rate. At room temperature of 300 K, GSs without defects show that brittle failure is at a low strain rate and linear hardening is at a high strain rate. The strain rate is higher, the GSs are harder. However, GSs with a large number of randomly distributed defects only show brittle failure under high temperature. The tensile strength and fracture strain increase with the strain rate increasing. The tensile strength of GSs without defects has a linear relation to the logarithm of the strain rate, but the GSs with defects do not exhibit this phenomenon because the defects are sensitive to the strain rate. The present study provides a theoretical optimization method for the preparation and performance of GSs.

Keywords Strain rate · Mechanical properties · Graphene sheets · Molecular dynamics simulations

1 Introduction

Graphene sheet (GS) is the representative material of carbon nanomaterial, which has attracted wide attention (Novoselov et al. 2004). Due to its superior mechanical, electrical, and thermal properties, GSs have spurred many new applications in materials enhancement, sensors, drug transportation, nanoelectronics, and nanodevices (Miao et al. 2014; Heersche et al. 2007; Zhou et al. 2014; Zhu and Ertekin 2014; Schmiedova et al. 2017; Levin et al. 2016; Jung et al. 2017; Singh et al. 2017). These applications are closely related to the mechanical properties of GSs. It has been illustrated that perfect GSs exhibit excellent mechanical properties. However, defects, such as atomic vacancy defects (Wang et al. 2012a), inevitably emerge in the preparation and synthesis of GS, which will greatly reduce the mechanical property (Zandiatashbar et al. 2014). Graphene sheets have physical properties such as impact resistance and high mechanical strength. Graphene sheet products have been widely used in the field of mechanical performance enhancement. Therefore, the study of the defective GS properties is important, and it is the basis for the application of a nanocomposite and nanometer device.

The numerical simulation method such as molecular dynamics (MD) is widely used in the mechanical properties investigation because of the conduction difficulty in nano-level and the discrete experimental data. Banhart et al. (2010) reviewed the possible structural defects on GSs and their potential applications. Another review on the fracture characteristics of GS was presented by Wang et al. (2012b). Song and Medhekar (2013) studied the tensile properties of GS with Stone–Wales effects by atomic simulation, the Stone–Wales effect on elastic modulus was not significant, and the defects only made GS anisotropy. Neek-Amal and Peeters (2010) used atomistic simulations to investigate the buckling of GS with randomly distributed vacancies; when subjected to axial stress, the buckling strain and mechanical stiffness decreased with the percentage of the defects. Zhao and Aluru (2010) used MD simulations to study the temperature effect and strain rate effect on the elastic modulus and strength of defective GS. They revealed that GS is a strong material even when subjected to variations in temperature, strain rate, and cracks. Mortazavi and Ahzi

✉ Shi Huan
13660767801@126.com

[1] School of Civil Engineering, Guangzhou University, Guangzhou 510006, People's Republic of China

[2] Earthquake Engineering Research Test Center, Guangzhou University, Guangzhou 510006, People's Republic of China

(2013) investigated the effects of different types of defects such as single-atom vacancy. Dewapriya et al. (2014) used MD simulations to study the effect of temperature on the crack propagation of GSs. Zhang and Zhang (2015) studied the effects of strain rate and temperature on the mechanical properties of the GSs with initial cracks by MD simulation.

On the other hand, many researchers (Kuang et al. 2015; Tserpes 2012) used the finite element method to investigate the elastic properties of the defective GSs. Although the finite element method can overcome the scale and time limit, as for the strain rate and temperature effects on the mechanical properties, MD simulation is still an effective and feasible method.

Throughout the current study on the mechanical properties of the defective GSs, only certain defects have been focused on. However, different percentages of randomly distributed defects may appear in the actual industrial manufacturing process. In this study, the effect of strain rate has been investigated on the mechanical properties of GSs, which contain different percentages of random defects by MD simulation, which include the effect of strain rate, different percentage defects on elastic modulus, tensile strength, ultimate strain, and so on.

2 Models and Simulation Methods

According to the size effects on the mechanical properties of GSs (Zhao et al. 2009), the size effect can be neglected when the diagonal of the square GS is larger than 5 nm; a 16 nm × 16 nm square GS with 9960 atoms is chosen as the initial perfect model which does not contain defects as shown in Fig. 1. In order to investigate the effects of the defects, randomly distributed vacancies in GS structure are created by a random numbers algorithm. One, 10, 50, 100, 200, and 500 atoms are randomly removed from the perfect GS, which is also called 0.01%, 0.1%, 0.5%, 1%, 2%, and 5% of the total atoms defects, respectively.

The simulation is conducted in a classical molecular dynamics code with the Large-scale Atomic/Molecular Massively Parallel Simulator (LAMMPS). A velocity Verlet (Chen et al. 2015) algorithm is used to integrate the equations of motion. The adaptive intermolecular reactive empirical bond-order potential (AIREBO), which had been proved reliable in the description of the GS, is adopted to describe the short-range covalent carbon bond interactions, the long-range van der Waals interaction (LJ terms), and torsion interactions (Stuart et al. 2000). In order to avoid abnormality at large deformation, the cutoff parameter for the short-range carbon bond interactions is chosen to be 2.0 (Liang et al. 2015).

Before dynamics simulation, a relaxation process has been implemented to minimize the total potential energy

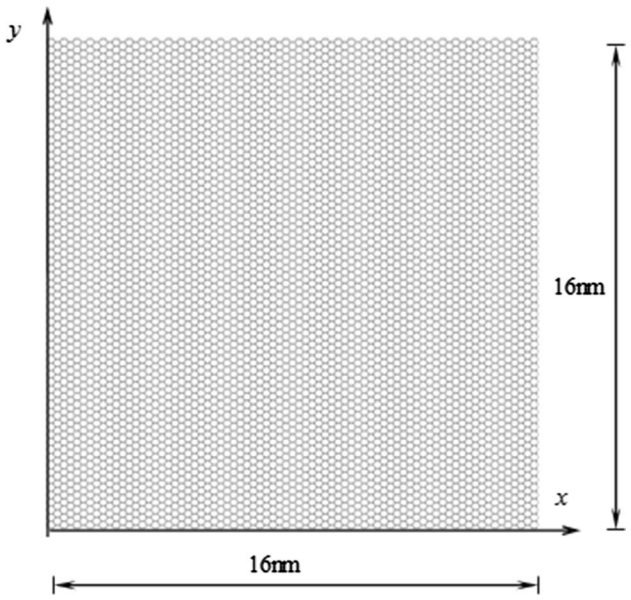

Fig. 1 Model of graphene sheet (perfect graphene sheet without defect)

of the entire GS, which enables the systems to be equilibrated at a certain temperature. In the process, the atoms around the vacancies will rearrange their local positions to balance the local stresses, and then, the system energy can achieve a stable initial state. After relaxing the initial configuration to obtain the minimum energy configuration, the GSs are stretched by applying external displacement on the atoms, while the other end is kept fixed. The displacement is applied systematically, the system is relaxed for a certain period to reach a new equilibrium state, and a new configuration can be obtained. The tension is carried out in a canonical ensemble, the so-called NVT. In order to clarify the strain rate effect on the mechanical properties, the simulation in the present study is carried out at different strain rates such as $0.5 \times 108\ s^{-1}$, $0.667 \times 108\ s^{-1}$, $1 \times 108\ s^{-1}$, and $2 \times 108\ s^{-1}$, which are applied by displacement of the atoms at the top end of the GSs. During the simulation, the Nose–Hoover thermostat is implemented to the equilibrium thermodynamic state at a certain constant temperature, such as 0.01 K, 300 K, 600 K, and 900 K, respectively.

3 Results and Discussion

The GSs with the width and the length of 16 nm were analyzed, which contain different distributed vacancies. Displacement in the *y*-direction is applied with four different strain rates. During each step of the simulation and stress–strain curves of the defected GSs, the position coordinates and stress of the atoms recorded can be obtained.

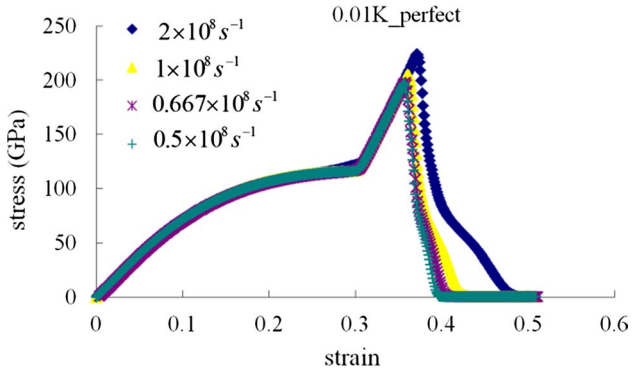

Fig. 2 Stress–strain curves of perfect graphene sheets at 0.01 K

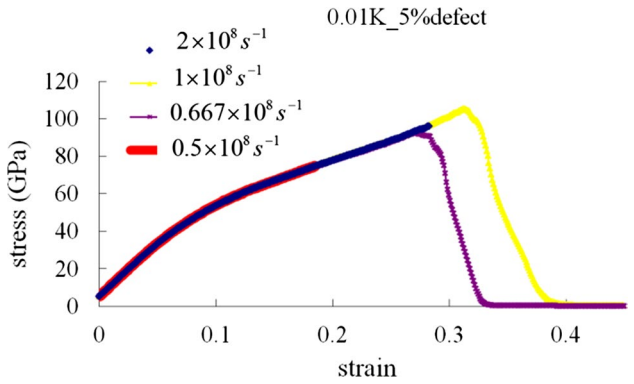

Fig. 3 Stress–strain curves of graphene sheets with 5% defect at 0.01 K

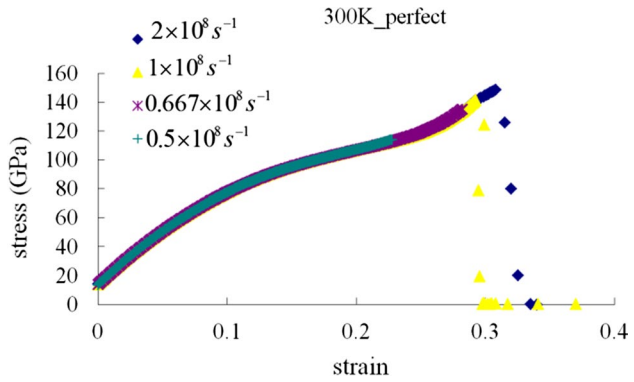

Fig. 4 Stress–strain curves of perfect graphene sheets at 300 K

Figures 2, 3, 4, and 5 show the stress–strain curves of GSs at different temperatures, different strain rates, and different percentages of defects. It can be seen that the stress–strain curves of GS with large number of defects (Fig. 3) are similar to Fig. 5, which are at high temperature. Figure 4 shows the stress–strain curves of perfect graphene sheets at 300 K. At first, the stress increases linearly with

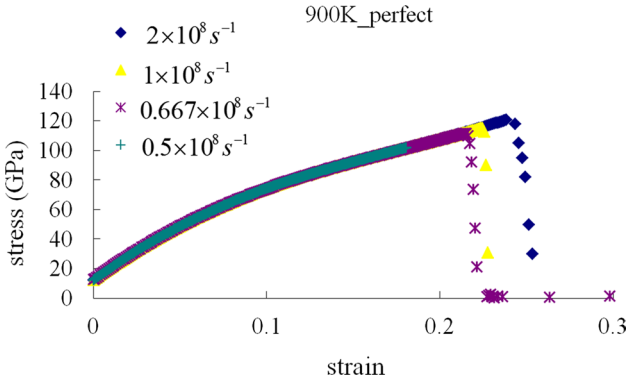

Fig. 5 Stress–strain curves of perfect graphene sheets at 900 K

the strain increasing due to the elastic deformation of carbon–carbon bonds. With the continuation of the stretching, the deformation is aggravated. Then, the stress quickens with the strain increasing with a nonlinear relation due to the nonlinear deformation of the carbon–carbon bond and the change in the bond angle. Finally, material is damaged when the ultimate stress is achieved. However, at temperature of 0.01 K, the stress–strain curve of GS without defects exhibits another property (see Fig. 2). The first two stages are the same as those of Figs. 3 and 5, and after the nonlinear stage, the GSs experience a linear strengthening process, in which the stress increases linearly with the strain increasing with a higher slope than that of the original linear stage, and then, fracture happens because of bond rupture. The tensile strength and the ultimate strain increase with the increase in the strain rate. The linear strengthening process greatly improves the strength of GSs.

In other words, the stress–strain curves exhibit two linear stages in the case of temperature 0.01 K. This result is similar to that obtained in the study (Sun et al. 2014). The first linear phase occurs in the elastic deformation of the carbon bond. The linear strengthening phase happens only in a few sets of acoustic modes, which are excited at very low temperatures, and most of the lattice vibrations are not excited. The heat exchanges less among the atoms, so it prolongs the lifetime of the carbon bond with the performance of a sharp rise. Higher strain rate means faster loading rate and less time for the atoms to exchange the heat and momentum. In that stage, the length of carbon bonds stretches at a high speed with less constraint and the carbon bonds are more difficult to destroy. So the higher the strain rate, the more the strength of the GS performance.

However, for the GSs with more defects, the temperature is very low, such as 0.01 K (Fig. 3), and there is no obvious linear strengthening process, which breaks the carbon bond by a large number of defects at an early stage. Accumulation of the broken bond would quickly lead to the rupture of the GSs. At the temperature of 300 K, the

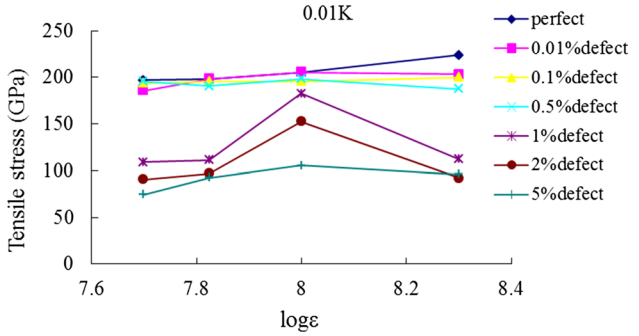

Fig. 6 The variation of tensile strength with strain rate at 0.01 K

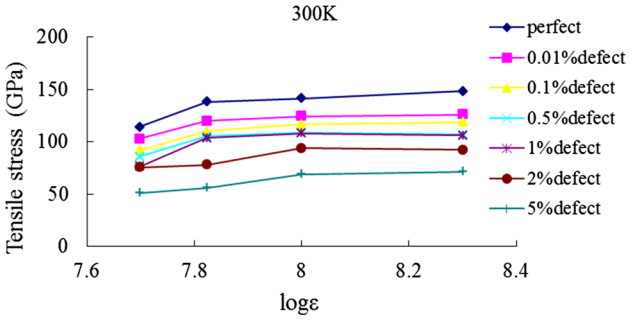

Fig. 7 The variation of tensile strength with strain rate at 300 K

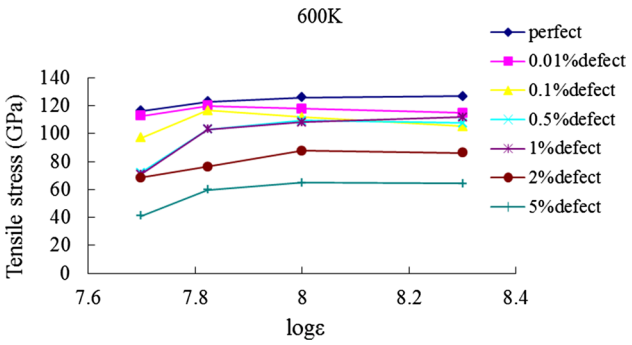

Fig. 8 The variation of tensile strength with strain rate at 600 K

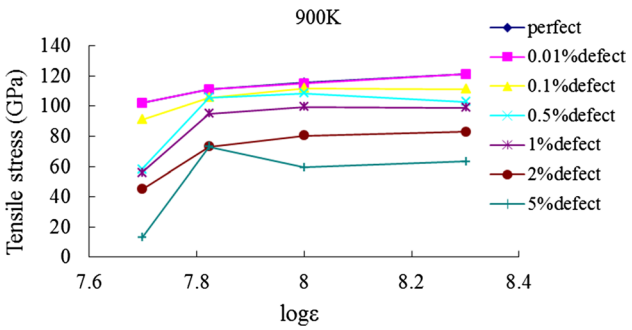

Fig. 9 The variation of tensile strength with strain rate at 900 K

GSs without defects rupture suddenly at low strain rate, which is the so-called brittle fracture. GSs show the linear strengthening process in the stress–strain relation when the strain rate is high enough. It can be seen from Fig. 4 that the brittle fracture occurs at the strain rate $0.5 \times 108\ s^{-1}$. However, the stress–strain curve has a slight linear strengthening process when the strain rate is higher than $0.667 \times 108\ s^{-1}$, which is a little bit like the GSs without defects at 0.01 K. The strength also increases with the increasing strain rate. The slight linear strengthening process replaces the obviously linear strengthening process by the effect of temperature. There are more lattice vibrations excited at the temperature of 300 K than 0.01 K, and the constraints for the changes in the carbon bond increased. Rather than extremely high temperature, the excited state is not so much, so the slightly strengthening process can be obtained. In addition, similar to that of 0.01 K, when the strain rate increased, the atoms cannot exchange the heat and momentum with each other on time, so the lifetime of the carbon bond can be prolonged. Hence, the higher strength with higher strain rate can be observed. It can be seen that when the strain rate is high enough, the failure mechanism of the GS will change.

When the strain rate is low, the atoms can exchange energy with each other fully, so only the GSs perform "brittle fracture." As temperature increases to 900 K, which is shown in Fig. 5, the GSs without defects do not appear at the linear strengthening stage at the high strain rate. As for the GSs with large percentage of defects, the defects are sensitive to the strain rates. As shown in Fig. 6, both the tensile strength and the ultimate strain increase with the increase in strain rate when the strain rate is less than $1 \times 108\ s^{-1}$ at 0.01 K. However, when the strain rate reaches $1 \times 108\ s^{-1}$, the tensile strength and ultimate strain decrease with increasing strain rate, the defects will break their nearby atoms b to form small cracks sooner with larger strain rate, and then these cracks will develop quickly with the strain rate increasing. So the tensile strength and ultimate strain decreasing with the strain rate increasing can be observed.

Figures 6, 7, 8, and 9 show the variation of tensile strength with the strain rate at different temperatures. As shown in Fig. 7, the tensile strength of GSs varies from 114 to 148 GPa at temperature of 300 K, which coincides with the result of tensile strength at 130 ± 10 GPa measured (Lee et al. 2008). It can be seen from Figs. 6 and 9 that the tensile strength of the GS without defects has linear relation to the logarithm of the strain rate even at different temperatures, in which the tensile strength increases with the increasing strain rate. This result is similar to that reported in the literature (Wang et al. 2013), in which the tensile strength of carbon nanotubes has a logarithmically linear relationship with

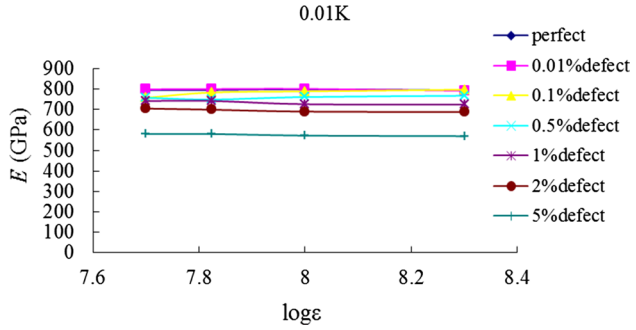

Fig. 10 The variation of elastic modulus with strain rate at 0.01 K

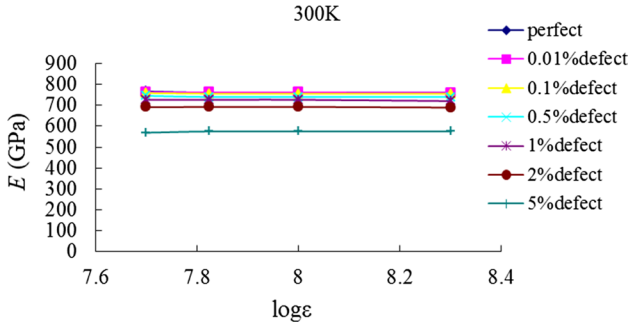

Fig. 11 The variation of elastic modulus with strain rate at 300 K

strain rate, and is also consistent with results of phase theory (Wang et al. 2013). The tensile strength decreases with the increasing percentage of the defects, and the tensile strength is no longer logarithmically linear with the strain rate. The tensile strength decreases with the increasing temperature.

It can be seen from Fig. 6 that there are the tensile strengths of GSs without defects or less, while the strain rate is increasing around 0.01 K, because the thermal effect can be ignored at the very low temperature. However, when the GSs contain more than 1% defects, the tensile strength first increases with the increase in strain rate, reaches its peak when strain rate logarithm is eight, and then decreases with the increase in strain rate. It is a fact that the defects are sensitive to the strain rate. The GSs containing more defects perform more sensitively. When the strain rate is high enough, more carbon–carbon bonds will be broken by the development of the defects, and the broken bond will accumulate quickly; then, the GS will soon reach its ultimate tensile strength. The tensile strength decreases with the increasing strain rate when GSs contain large percentage of defects.

When the temperature is higher than 0.01 K, the thermal motion becomes one main factor that affects the tensile strengths, and the effects of both strain rate and temperature will make the variation of the tensile strength by the different strain rates. In some conditions, tensile strength increases with the increasing strain rate, and some increase first and then decrease; the extreme position depends on the temperature and the percentage of the defects.

Figures 10, 11, 12, and 13 show the variation of the elastic modulus with strain rate at different temperatures. In Fig. 11, the elastic modulus of GS without defects at room temperature (300 K) is about 760 GPa, which coincides with that of the literature (Ansari et al. 2012; Sadeghi Nik et al. 2010) from 600 to 1200 GPa.

It can be observed from Figs. 10, 11, 12, and 13 that the variations of elastic modulus with the strain rate are almost a straight line irrespective of different temperatures, in other words, elastic modulus is independent of the strain

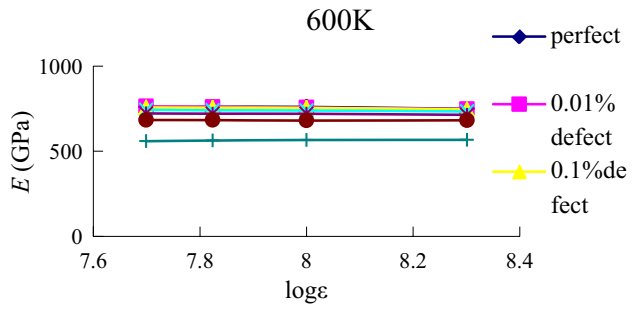

Fig. 12 The variation of elastic modulus with strain rate at 600 K

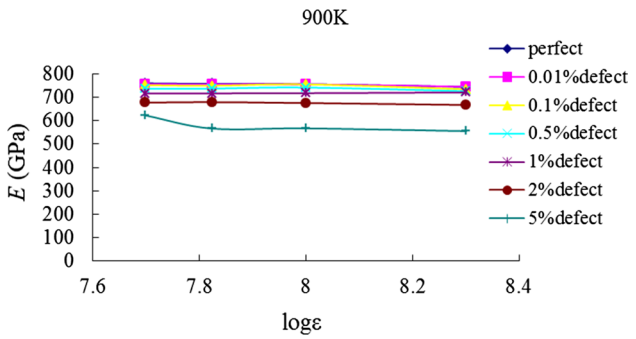

Fig. 13 The variation of elastic modulus with strain rate at 900 K

rate, and the effect of the strain rate on the elastic modulus is small. Figure 12 shows the variation of elastic modulus with strain rate at 600 K. The elastic modulus decreases with the increase in the defects. The elastic modulus of the GSs without defects is the largest. In addition, the GSs contain more defects and the elastic modulus is smaller. The degree of decreasing is related to the temperature. For example, the elastic modulus of 5% defective GS is lower than that of the 28% GS without defects when the temperature is around 0.01 K. Moreover, the amount of reduction is about 25% when the temperatures are 300 K, 600 K, and 900 K. It can be seen that the percentage of the reduction is the most

except the lower temperature. However, if the temperature is above room temperature, the reduction in the elastic modulus by the defects is almost the same according to different temperatures. It can also be observed that the elastic modulus decreases with the increasing temperature.

4 Conclusion

In this study, using molecular dynamics simulations, the mechanical properties of GSs were investigated by a different percentage of random defects. The interaction of carbon and carbon bonds has been described by AIREBO potential. The strain rate effects are analyzed on tensile strength, ultimate strain, and elastic modulus. The results show that the strain rate has a significant effect on the deformation characteristics, tensile strength, and ultimate strain of GSs, which has little effect on the elastic modulus. The stress–strain curves of the GSs without defects exhibit two linear stages, which are the elastic deformation stage and the linear strengthening stage in the case of temperature 0.01 K. The first linear stage happens at the elastic deformation of the carbon bond. The linear strengthening stage is compatible with the fact that most of the lattice vibrations are not excited at very low temperature. The strain rate is higher; the linear strengthening stage is more obvious. As for room temperature of 300 K, the GSs without defects rupture suddenly at low strain rate and have the linear strengthening process in the stress–strain relation when the strain rate is high enough. When the strain rate is high enough, the failure mechanism of the GSs will change. The process of strengthening linear does not appear; when the percentage of the random defects is large or the temperature is high enough, the GSs only show brittle damage. The tensile strength and ultimate strain increase with the increasing strain rate. The tensile strengths of the GSs without defects are approximately linear with the logarithm of the strain rate, but those of the defective GSs do not exhibit this relation by the defect sensitivity to strain rate.

Acknowledgements The authors wish to acknowledge the support from the National Natural Science Foundation of China (Grant No. 11702067), Guangdong Province (Grant No. 2016A030313617), and the Foundation for Young Talents in Higher Education of Guangdong (Grant No. 2015KQNCX122).

References

Ansari R, Ajori S, Motevalli B (2012) Mechanical properties of defective single-layered graphene sheets via molecular dynamics simulation. Superlattices Microstruct 51(2):274–289

Banhart F, Kotakoski J, Krasheninnikov AV (2010) Structural defects in graphene. ACS Nano 5(1):26–41

Chen MQ, Quek SS, Sha ZD et al (2015) Effects of grain size, temperature and strain rate on the mechanical properties of polycrystalline graphene—a molecular dynamics study. Carbon 85:135–146

Dewapriya MAN, Rajapakse RKND, Phani AS (2014) Atomistic and continuum modelling of temperature-dependent fracture of graphene. Int J Fract 187(2):199–212

Heersche HB, Jarillo-Herrero P, Oostinga JB, Vandersypen LMK, Morpurgo AF (2007) Bipolar supercurrent in graphene. Nature 446(7131):56–59

Jung GS, Yeo J, Tian ZT, Qin Z, Buehler MJ (2017) Unusually low and density-insensitive thermal conductivity of three-dimensional gyroid graphene. Nanoscale 9(36):13477–13484

Kuang Y, Lindsay L, Huang B (2015) Unusual enhancement in intrinsic thermal conductivity of multi layer graphene by tensile strains. Nano Lett 15(9):6121–6127

Lee C, Wei X, Kysar JW, Hone J (2008) Measurement of the elastic properties and intrinsic strength of monolayer graphene. Science 321(5887):385–388

Levin DD, Bobrinetskiy II, Emelianov AV, Nevolin VK, Romashkin AV, Petuhov VA (2016) Surface functionalization of single-layer and multilayer graphene upon ultraviolet irradiation. Semiconductors 50(13):1738–1743

Liang Y, Han Q, Huan S (2015) The effects of temperature and vacancies on the elastic modulus and strength of graphene sheet. J Therm Stresses 38(8):926–933

Miao T, Yeom S, Wang P, Standley B, Bockrath M (2014) Graphene nanoelectromechanical systems as stochastic-frequency oscillators. Nano Lett 14(6):2982–2987

Mortazavi B, Ahzi S (2013) Thermal conductivity and tensile response of defective graphene: a molecular dynamics study. Carbon 63:460–470

Neek-Amal M, Peeters FM (2010) Defected graphene nanoribbons under axial compression. Appl Phys Lett 97(15):153118

Novoselov KS, Geim AK, Morozov SV, Jiang D, Zhang Y, Dubonos SV, Grigorieva IV, Firsov AA (2004) Electric field effect in atomically thin carbon films. Science 306(5696):666–669

Sadeghi Nik A, Bahari A, Ebadi AG, Ghasemi-Hamzekolaee A (2010) The role of nano particles (Si) in gate dielectric. Indian J Sci Technol 3(6):634–636

Schmiedova V, Pospisil J, Kovalenko A, Ashcheulov P, Fekete L, Cubon T, Kotrusz P, Zmeskal O, Weiter M (2017) Physical properties investigation of reduced graphene oxide thin films prepared by material inkjet printing. J Nanomater 2017:3501903

Singh D, Kumar A, Kumar D (2017) Adsorption of small gas molecules on pure and Al-doped graphene sheet: a quantum mechanical study. Bull Mater Sci 40(6):1263–1271

Song J, Medhekar NV (2013) Thermal transport in lattice-constrained 2D hybrid graphene heterostructures. J Phys Condens Matter 25(44):445007

Stuart SJ, Tutein AB, Harrison JA (2000) A reactive potential for hydrocarbons with intermolecular interactions. J Chem Phys 112(14):6472–6486

Sun YJ, Huang YH, Ma F, Ma DY, Hu TW, Xu KW (2014) Molecular dynamics simulation on double-elastic deformation of zigzag graphene nanoribbons at low temperature. Mater Sci Eng B Adv Funct Solid State Mater 180:1–6

Tserpes KI (2012) Strength of graphenes containing randomly dispersed vacancies. Acta Mech 223(4):669–678

Wang MC, Yan C, Ma L, Hu N, Chen MW (2012a) Effect of defects on fracture strength of graphene sheets. Comput Mater Sci 54:236–239

Wang L, Chen Z, Dean CR, Taniguchi T, Watanabe K, Brus LE, Hone J (2012b) Negligible environmental sensitivity of graphene in a hexagonal boron nitride/graphene/h-BN sandwich structure. ACS Nano 6(10):9314–9319

Wang X, Huang T, Lu S (2013) High performance of the thermal transport in graphene supported on hexagonal boron nitride. Appl Phys Express 6(7):075202

Zandiatashbar A, Lee G-H, An SJ, Lee S, Mathew N, Terrones M, Hayashi T, Picu CR, Hone J, Koratkar N (2014) Effect of defects on the intrinsic strength and stiffness of graphene. Nat Commun 5:3186

Zhang G, Zhang Y-W (2015) Strain effects on thermoelectric properties of two-dimensional materials. Mech Mater 91:382–398

Zhao H, Aluru NR (2010) Temperature and strain-rate dependent fracture strength of graphene. J Appl Phys 108(6):064321

Zhao H, Min K, Aluru NR (2009) Size and chirality dependent elastic properties of graphene nanoribbons under uniaxial tension. Nano Lett 9(8):3012–3015

Zhou H, Zhu J, Liu Z, Yan Z, Fan X, Lin J, Wang G, Yan Q, Yu T, Ajayan PM, Tour JM (2014) High thermal conductivity of suspended few-layer hexagonal boron nitride sheets. Nano Res 7(8):1232–1240

Zhu T, Ertekin E (2014) Phonon transport on two-dimensional graphene/boron nitride superlattices. Phys Rev B 90(19):195209